CHAPTER 66

DISTRIBUTION OF UNDERTOW AND LONG-WAVE COMPONENT VELOCITY DUE TO RANDOM WAVES

Akio Okayasu[1] and Hiroyuki Katayama[2]

Abstract

Laboratory measurements were performed on cross-shore velocity variations in the surf zone caused by random waves by using a laser Doppler velocimeter. Two-dimensional distributions of undertow and long-wave component velocity were obtained on a uniform slope bed and a bar-type beach. A model was presented to estimate undertow distribution due to random waves on an arbitrary beach topography.

1. Introduction

In order to predict the sediment transport and the material diffusion in the surf zone, it is necessary to evaluate the velocity distribution of undertow with high accuracy. In the last decade, many detailed laboratory measurements related to the velocity distribution in the surf zone were performed under regular wave conditions [see e.g. Stive and Wind (1982), Nadaoka and Kondoh (1982) and Okayasu *et al.* (1986)]. In these researches, it was pointed out that the characteristics of waves and velocity fields change significantly around breaking or plunging points. The mass flux due to waves and vertical profiles of undertow also differ between the outer and inner region of the surf zone. On the basis of the experimental results, some theoretical and numerical models have been presented to estimate the undertow distribution by, such as, Svendsen (1984), Nadaoka and Hirose (1986), Tsuchiya *et al.* (1988) and Okayasu *et al.* (1990).

[1] Research Associate, Department of Civil Engineering, Yokohama National University, Hodogaya-ku, Yokohama 240, Japan

[2] Graduate Student, Department of Civil Engineering, Yokohama National University, Hodogaya-ku, Yokohama 240, Japan

However, the actual wave field is random. Velocity measurements under random wave conditions and models based on them are needed for practical use. Sato *et al.* (1988) performed laboratory measurements of near-bottom velocity in the surf zone under random wave conditions by using a laser Doppler velocimeter (LDV). Isobe (1983) and Mckee Smith *et al.* (1992) measured nearshore velocity in the filed, then investigated the vertical distribution of cross-shore steady current. However, the number of measuring points was not enough for the quantitative discussion.

In the present study, laboratory experiments were performed for random wave conditions to measure cross-shore velocity in the surf zone by using LDV. The beach topographies were a 1/20 constant slope and a bar-type beach. Then a model was investigated to estimate the undertow distribution due to random wave breaking on an arbitrary beach topography by applying a model for regular wave conditions.

In recent years, the importance of long-wave component velocity on the sediment transport have been recognized in and near the surf zone, especially in terms of the suspended sediment transport. In this study, the velocity distribution of long-wave component in the surf zone is also investigated.

2. Experimental arrangements

The experiments were performed in a wave flume which was 17 m long and 0.5 m wide. A random wave generator with absorption control for reflected waves was equipped at one end of the flume. Beach topographies were a 1/20 uniform slope and a bar-type beach. The bar-type beach consisted of the first 5 m of 1/20, the next 1 m of $-1/20$ and the last 4 m of 1/20 slopes. The bottom of the slopes were smooth. The figure 1 shows the side view of the flume with the bar-type beach.

Regular and random incident waves were used for the case of uniform slope beach to investigate the difference in the velocity field. The random waves (case 1) had the Bretshneider-Mitsuyasu spectrum and the significant wave height and period were planed to be almost same values as the wave height and period of the regular waves (case 2). In cases 3 and 4, velocity was measured on a bar-type beach for two random waves which had different significant wave heights and periods. The waves broke just before the top of the bar in case 3, and they began to break offshoreward away from the bar in case 4. The still water depths in the offshore regions, h_i, were 35.0 cm in cases of the uniform slope and 32.0 cm for the bar-type. The water depth at the top of the bar was 7.0cm. The experimental conditions are listed in Table 1. In the table, T is the wave period, H_i the wave height in the offshore region. For random waves, they are noted as the values for significant waves analyzed by using the zero-down cross method.

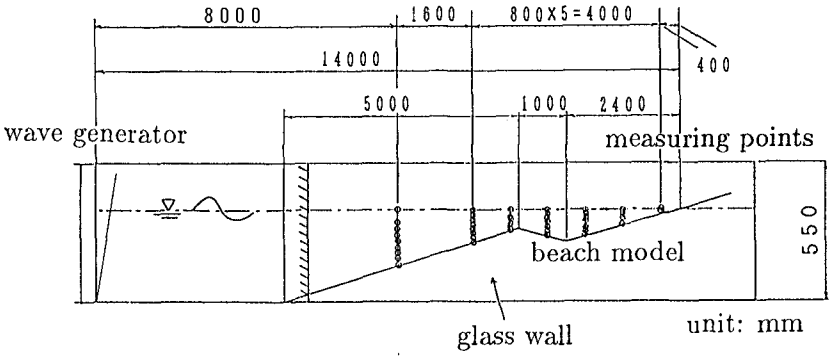

Fig. 1 Side view of the flume (bar-type beach).

Table 1 Experimental conditions

case	beach type	h_i (cm)	T (s)	H_i (cm)	wave condition
1	uniform	35.0	1.20	7.85	regular
2	uniform	35.0	1.26	8.28	random
3	bar-type	32.0	0.945	5.67	random
4	bar-type	32.0	1.14	7.52	random

Seven vertical measuring lines were set on the beach model in each case, which covered the whole surf zone. Along these lines, several measuring points were arranged vertically from 2 mm above the bottom to the mean water level in every 3 to 40 mm. The distance from the points to the side wall of the flume was 16 cm. The total number of the measuring points were 49 for the uniform slope beach and 53 for the bar-type beach. The x-axis and z-axis were set to be onshoreward and vertically upward, respectively. The origin of the co-ordinates was the shoreline at the still water level.

An one-component LDV (15 mW, He-Ne) was used to measure the cross-shore velocity. The data of water surface elevation above the measuring point were also taken simultaneously by using a capacitance-type wave gage. The velocity and wave profile data were sampled every 20 ms and were stored in a digital data recorder.

For regular wave condition (case 1), the ensemble mean value of velocity was obtained as the average at the same phase of waves over 100 wave period. The steady current was calculated from those ensemble mean values. In case of random wave conditions, data were recorded for 5 minute (3 minute for case 2) after 3 minute of wave generating to make the wave field steady in every measurement. When the velocity was repeatedly measured at each point, the same incident signal for random waves was used in each case.

The long-term gradual fluctuation of the output voltage from the LDV system may seriously affect the precision of the velocity measurement, especially for the steady current, because the value of steady current is usually far smaller than the amplitude of the orbital velocity by waves. Therefore, the output signal from the LDV system in the still water condition was recorded for every measuring point and was used to compensate the zero level of the recorded velocity.

3. Experimental results

In random wave conditions, the cross-shore velocity u and the water surface elevation η can be divided into 4 components in terms of frequency f. They are, steady components U and $\overline{\eta}$, long-wave components u_l and η_l, short-wave components u_s and η_s and turbulence components u_t and η_t. In the present study, u_l and η_l were defined as $f < 0.3$ (Hz), u_s and η_s as $0.3 \leq f < 5$ (Hz) and u_t and η_t as $5 \leq f$ (Hz). They were obtained by using numerical filters.

3.1 Distribution of undertow

Figure 2 shows the results of steady current distribution on the uniform slope. The distributions for regular wave condition and that of random wave condition are shown together. In the figure, "b.p." denotes the breaking point by regular waves, "b.p.$_{1/3}$" denotes the significant breaking point due to random waves. Since these breaking points were determined on the measuring lines where the wave height or the significant wave height take their maximum values, the exact points of wave breaking may be different within the neighboring measuring lines. The mean water level due to regular waves is indicated in the figure.

In case of regular waves, the vertical profiles abruptly change a little after the wave breaking ($x = -180$ to -120 in Fig. 2). On the contrary, profiles near breaking point show gradual change in their forms for the random wave condition. The reason should be because that the positions of breaking have a variation in the cross-shore direction. The change already takes place from the breaking point in the case of random waves. This means that the influence by large waves in random condition cannot be neglected on the steady current distribution, although the frequency in appearance of the large waves is small.

No significant difference in the profiles is found in the inner region where almost all waves break. Vertically averaged values of undertow in random wave condition are 10 % or 30 % smaller than those by regular waves with equivalent wave heights.

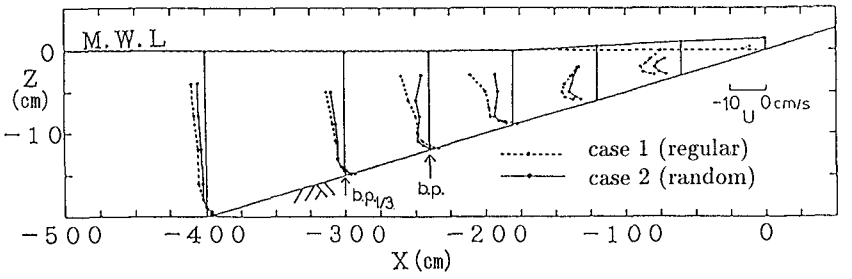

Fig. 2 Measured undertow due to regular and random waves (uniform slope).

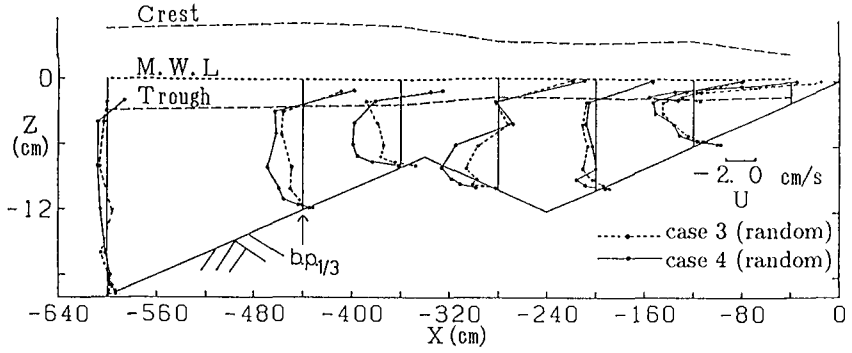

Fig. 3 Measured undertow due to random waves (bar-type).

Figure 3 gives the undertow distributions on the bar-type beach. In the figure, the mean water level for case 4 is shown. The crest and trough levels were obtained by averaging those of 1/3 maximum waves. In these cases, waves break around the top of the bar. At the onshoreside slope of the bar, the distribution shows the typical profiles for inner region which has strong offshore directed current near the bottom.

After the first breaking, waves recover at the trough of the bar. The undertow profiles there become similar to the profiles outside the surf zone. The near-bottom velocity is offshoreward at the top of the bar, however, it comes onshoreward again at the trough. It can be considered that the bottom boundary layer develops at the trough of the bar.

3.2 Distribution of long-wave component velocity

Figure 4 shows the two-dimensional distribution of long-wave component of velocity, which was extracted by using a numerical filter from the time series of measured velocity. The root-mean-square value $u_{l\,\mathrm{rms}}$ of the low frequency component velocity u_l on the uniform slope is given in the figure.

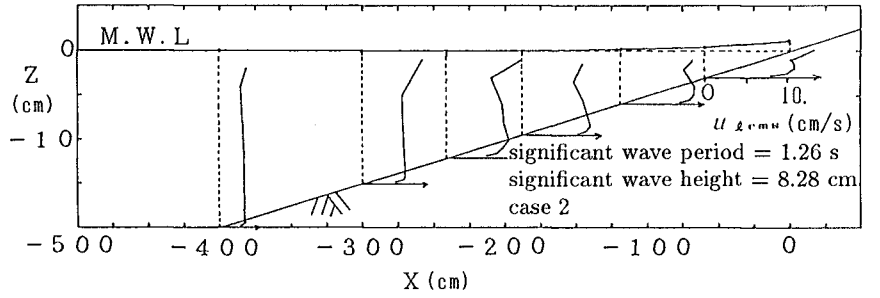

Fig. 4 RMS Value of long-wave component velocity (uniform slope).

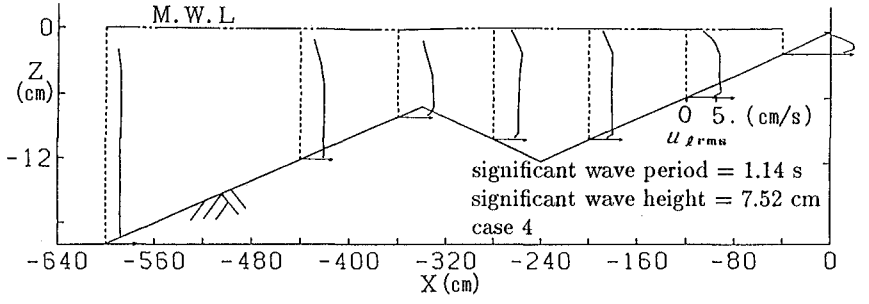

Fig. 5 RMS value of long-wave component velocity (bar-type).

The distribution of $u_{l\,\mathrm{rms}}$ on the bar-type beach is shown in Fig. 5. In both cases, the amplitudes of long-wave component are almost constant in vertical direction same as the distribution of the short-wave component, although the figures show maximum values around the elevation of 1 cm from the bottom. Below the level, the amplitudes considerably decrease. It should be due to the bottom boundary layer, but probably it is different from the ordinary turbulent oscillatory boundary layer because of the turbulence from the upper layer produced by wave breaking.

Figure 6 gives distribution of vertically averaged values u_{lm} of $u_{l\,\mathrm{rms}}$ on the bar-type beach. The variation of root-mean-square value $\eta_{l\,\mathrm{rms}}$ of low-frequency component of water surface elevation is shown together. Both of them take large values at the top of the bar, then decrease a little with increasing water depth in wave recovery zone, and then increase remarkably after second wave breaking. This result supports the previous researches for cross-shore variations of the long-wave components.

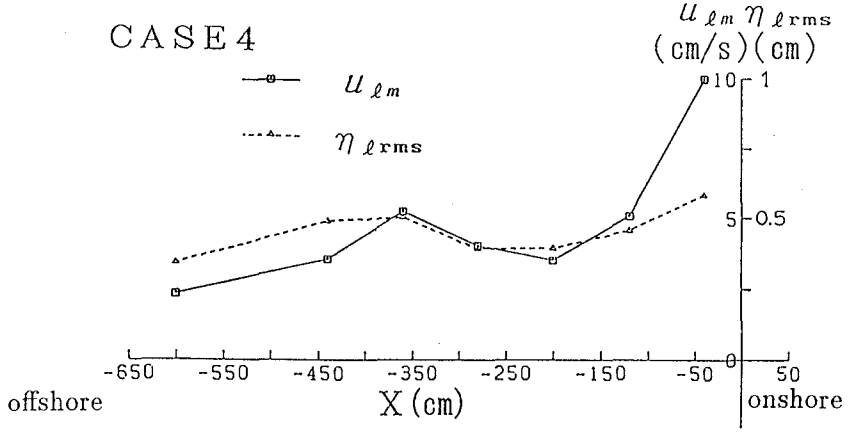

Fig. 6 Cross-shore variation of long-wave component velocity (bar-type).

4. Undertow Model for Random Wave Condition

In random wave condition, the spatial distribution of breaking points cause gradual change of undertow profile around the break points as shown in the section 3.1. Therefore, in this case, good accuracy near the breaking points cannot be expected to undertow models developed for regular wave conditions.

In the present study, a model was investigated to estimate the undertow profile under random wave breaking by applying a model for regular waves.

In order to obtain the undertow distribution due to random waves by using a model for regular waves, it may be possible to estimate the distribution by superimposing the calculated values for every individual wave in the time series of random waves. However, it should not be practical because this way must need much computing time. Therefore, representative wave heights which were obtained by using the individual wave analysis was used in this study.

At first, individual offshore measured waves are classified into three groups which contain 1/10 of the highest, 7/30 of the next highest and 2/3 of the rest, that is the lowest waves. Then, the average wave heights H_1, H_2 and H_3 for each group are calculated. The values H_1, H_2 and H_3 are easily obtained by using the relations as shown below from the 1/10 maximum wave height $H_{1/10}$, the significant wave height $H_{1/3}$ and the mean wave height $\overline{H}$.

$$H_1 = H_{1/10}$$

$$H_2 = \frac{10H_{1/3} - 3H_{1/10}}{7} = 1.429H_{1/3} - 0.429H_{1/10}$$

$$H_3 = \frac{3\overline{H} - H_{1/3}}{2} = 1.5\overline{H} - 0.5H_{1/3}$$

The each value is put into the undertow model presented by Okayasu *et al.* (1990) for regular wave conditions as the incident wave condition to evaluate the undertow distribution due to the representative waves. U_1, U_2 and U_3 are calculated undertow value from H_1, H_2 and H_3 with the significant wave period T. Contributions by the three representative waves were estimated by multiplying the factor of 1/10, 7/30 and 2/3 which are the frequencies of appearance of the each obtained values. Finally, the contributions are linearly superimposed and the undertow distribution due to the random waves is obtained. Figure 7 gives the flow chart of this process.

The calculated undertow distribution on the uniform slope is shown in Fig. 8 with the measured distribution. The calculated profile changes gradually around the breaking point.

Figure 9 shows the distribution on the bar-type beach. The overall agreement is good. The model can evaluate the profiles also in wave recovery zone, especially for onshore directed flow in the vicinity of the bottom. It can be said that the model is able to estimate the undertow distribution due to random waves.

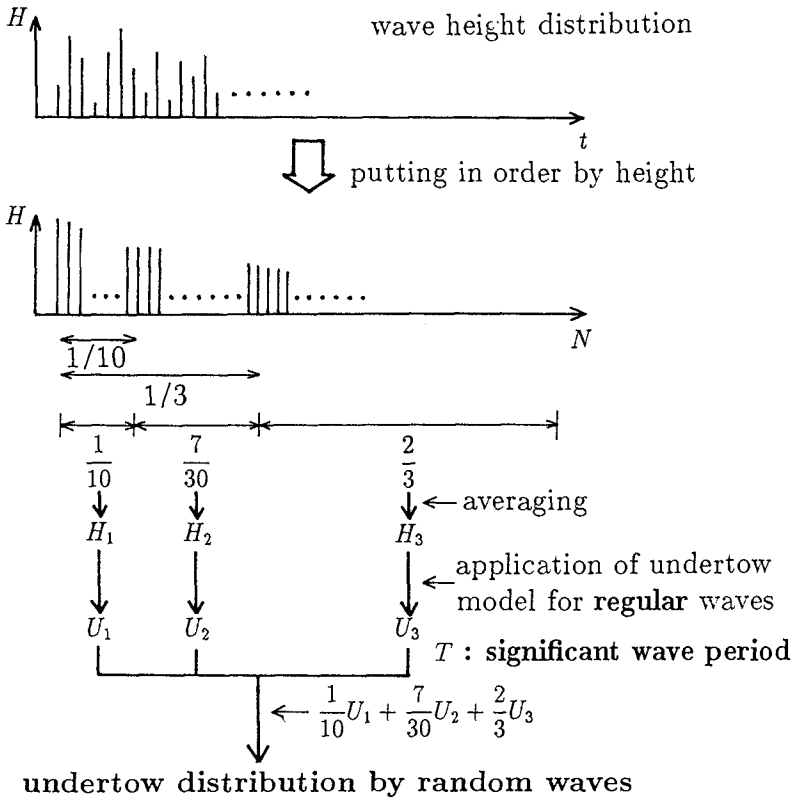

Fig. 7 Flow chart of the process of undertow evaluation.

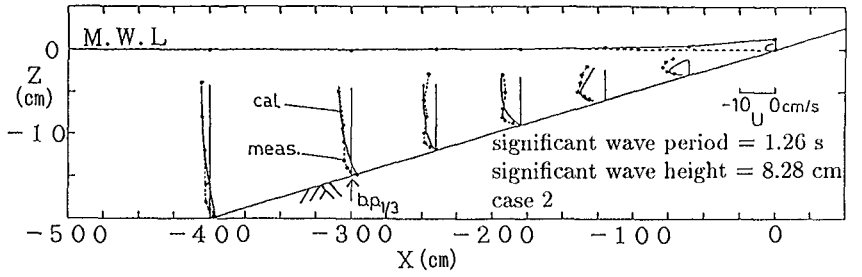

Fig. 8 Calculated and measured undertow (uniform slope).

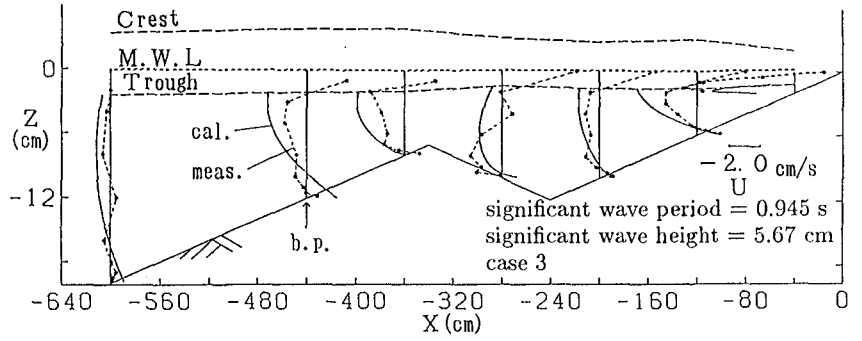

Fig. 9 Calculated and measured undertow (bar-type).

5. Conclusions

In the present study, laboratory experiments were performed for random wave conditions to measure cross-shore velocity in the surf zone on a 1/20 constant slope and a bar-type beach. Then a model was formulated to estimate undertow distribution caused by random wave breaking on arbitrary beach topographies from the offshore wave height distributions. The vertical distribution of long-wave component velocity was also investigated.

The conclusions obtained in this study are as follows.

1) The vertically averaged values of undertow due to random waves are 10 to 30 % smaller than those by regular waves. The change of vertical profiles of

undertow in the cross-shore direction around the breaking point is gradual under random wave conditions.

2) The amplitude of long-wave component velocity can be considered almost constant in vertical direction, although the influence by the boundary layer is obvious in the vicinity of the bottom.

3) The distribution of undertow caused by random waves can be estimated from three representative wave heights obtained from offshore wave height distribution. The distributions for the three representative wave heights calculated by using a model for regular waves are superimposed with factors depending on the frequencies of appearance.

References

Isobe, M., 1983: Field observation of vertical distribution of mean velocity in the nearshore zone, *NERC Rep.*, No.17, TR–82–1, pp.66–73 (in Japanese).

Mckee Smith, J., I.A. Svendsen and U. Putrevu, 1992: Vertical structure of the nearshore current at DELILAH: measured and modeled, *Abstracts 23rd Int. Conf. Coastal Eng.*, pp.156–157.

Nadaoka, K. and F. Hirose, 1986: A modeling of water particle dispersion under breaking waves in the surf zone, *Proc. 33rd Japanese Conf. Coastal Eng.*, pp.26–30 (in Japanese).

Nadaoka, K. and T. Kondoh, 1982: Laboratory measurements of velocity field structure in the surf zone by LDV, *Coastal Eng. Japan*, JSCE, Vol.25, pp.125–145.

Okayasu, A., T. Shibayama and N. Mimura, 1986: Velocity field under plunging waves, *Proc. 20th Int. Conf. Coastal Eng.*, pp.660–674.

Okayasu, A., A. Watanabe and M. lsobe, 1990: Modeling of energy transfer and undertow in the surf zone, *Proc. 22nd Int. Conf. Coastal Eng.*, pp.123–135.

Sato, S., M. Fukuhama and K. Horikawa, 1988: Measurements of near-bottom velocities in random waves on a constant slope, *Coastal Eng. Japan*, JSCE, Vol.31, No.2, pp.219–229.

Stive, M.J.F. and H.G. Wind, 1982: A study of radiation stress and set-up in the near-shore region, *Costal Eng.*, Vol.6, pp.1–25.

Svendsen, I.A., 1984: Mass flux and undertow in a surf zone, *Coastal Eng.*, Vol.8, pp.347–365

Tsuchiya, Y., T. Yamashita and M. Uemoto, 1988: A model of undertow in the surf zone, *Coastal Eng. in Japan*, Vol.30, No.2, pp.63–73.